SUPPLEMENTARY APPENDIX FOR THE STUDY:

ATP dynamics as a predictor of future podocyte structure and function after acute ischemic kidney injury

Table of contents

Supplementary Figure 1

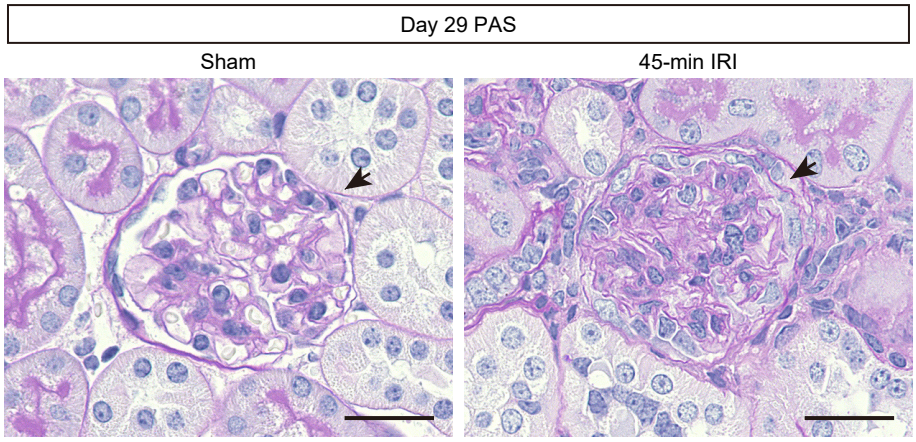

Supplementary Figure 1. Representative images of periodic acid-Schiff (PAS) staining of glomeruli 29 days after 45-min IRI and sham surgery. Arrowheads indicate glomeruli. Scale bars: 20 μm. PAS, periodic acid-Schiff.

Supplementry Figure 2

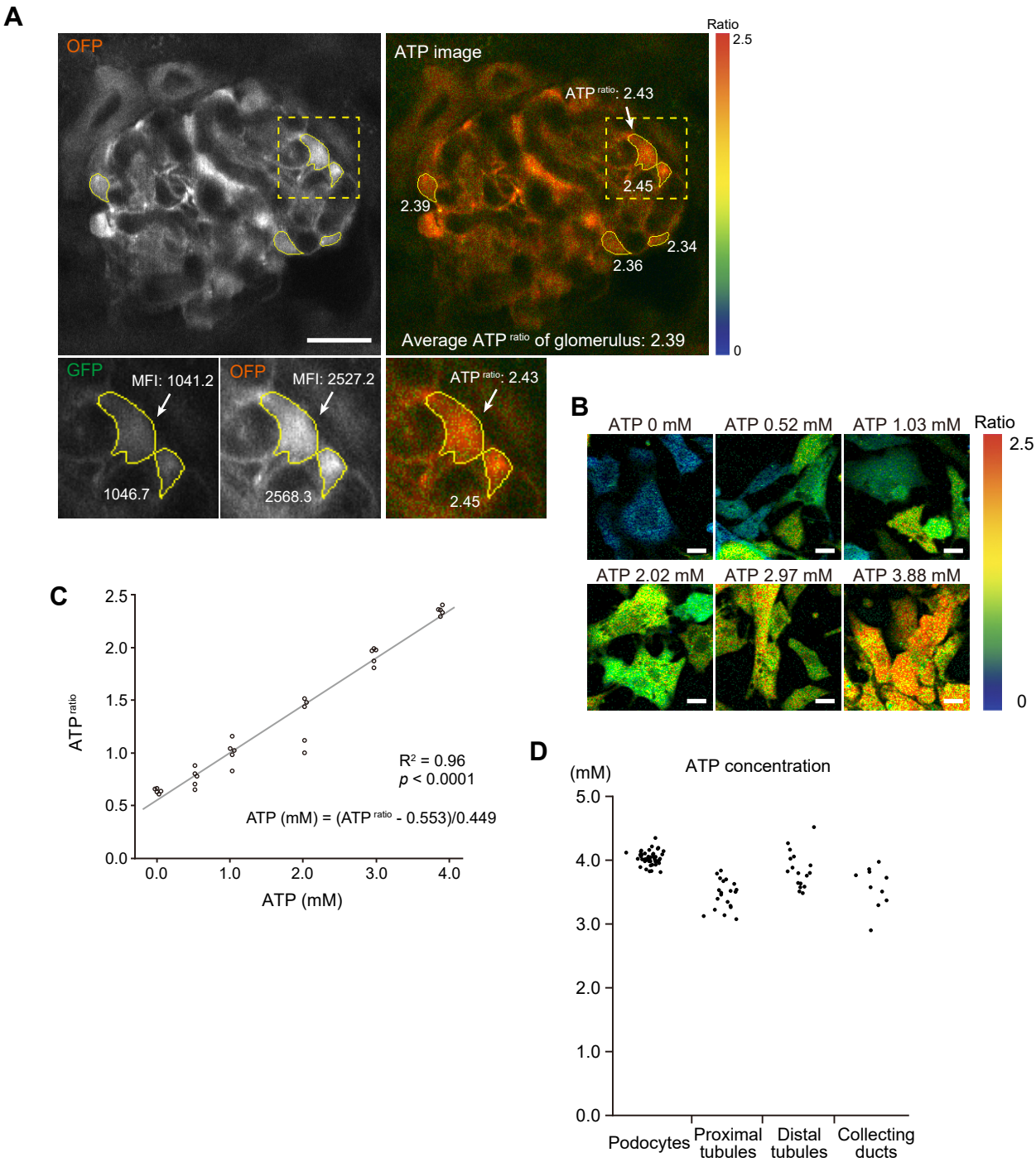

Supplementary Figure 2. ATP ratio measurement for podocytes and estimation of actual intracellular ATP concentration.
(A) Sample images of the procedure for creating regions of interest in OFP and GFP images (left images) and ATP images (right images). Regions of interest were created in OFP images and transferred to GFP images to determine mean fluorescent intensity (MFI) in the regions of interest. The ATP ratio of each region of interest was determined by dividing OFP-MFI by GFP-MFI. In each glomerulus, at least four podocytes that had clear signals were selected for analysis. Areas in the dashed boxes are magnified in the lower images. (B) ATP images of primary cultured GO-ATeam2 MEFs with arbitrary ATP concentrations. (C) Association between ATP ratio and actual ATP concentration in primary cultured GO-ATeam2 MEFs. Each dot represents a value of each cell. Overlapping dots are manually shifted aside for clarity. ATP ratio was measured at following ATP concentrations: 0.0, 0.52, 1.03, 2.02, 2.97, 3.88 mM. Correlation was determined using a Pearson's correlation analysis. (D) Estimated ATP concentrations in podocytes and tubules. Data set is the same with Figure 2E. Scale bars: 20 μm in A and B. MFI, mean fluorescent intensity.

Supplemental Figure 3

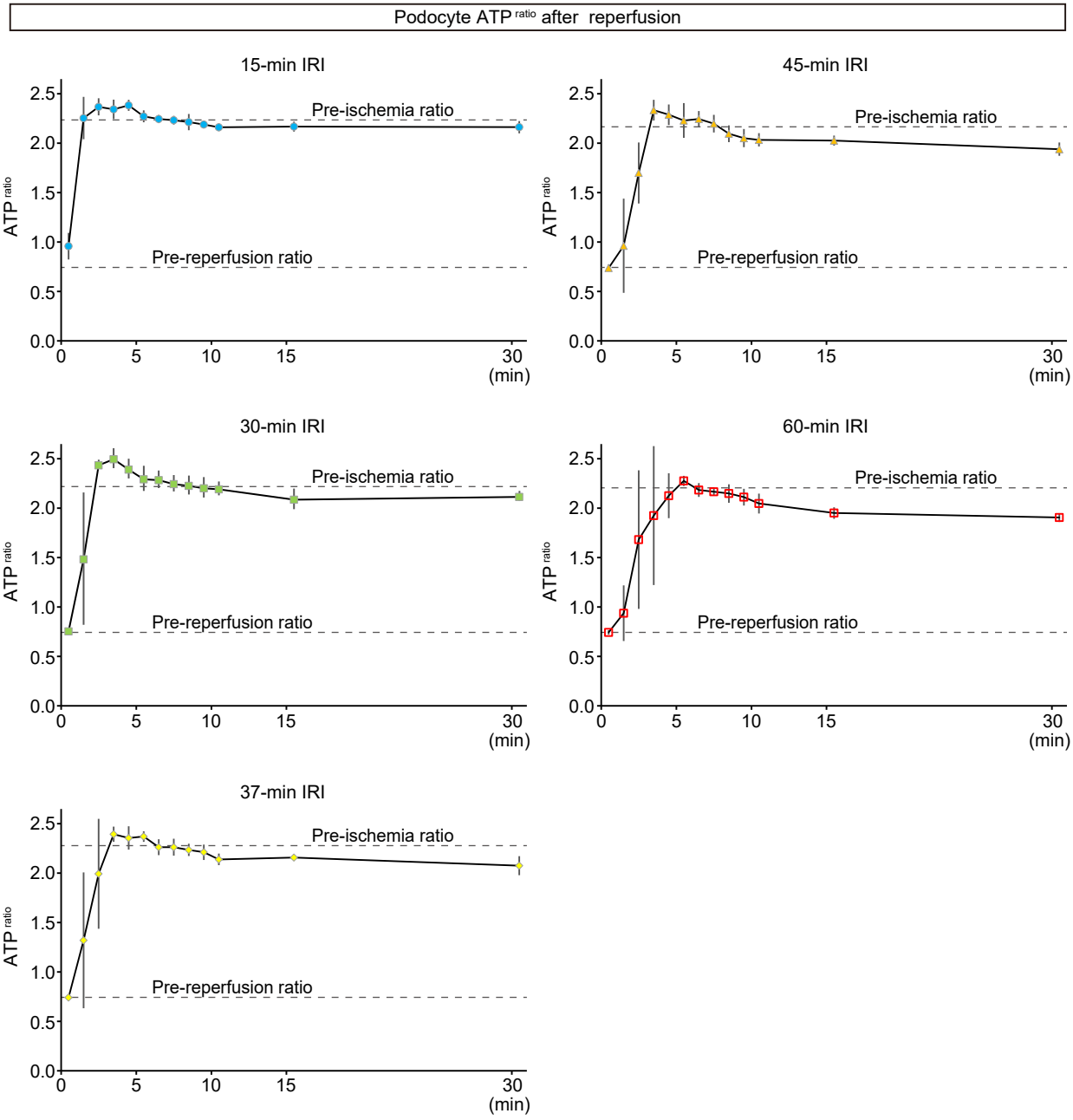

Supplementary Figure 3. Podocyte ATP ratio after reperfusion. The time-course changes of ATP ratio after different ischemia severities are shown separately. The average ATP ratios in at least four podocytes in one glomerulus for each time point were used to determine the ATP ratio for each mouse. The mean ATP ratio in each group was shown as a dot at each timepoint (n=4 mice per group). The average of basal ATP ratio before ischemia in each group and the lowest ATP ratio before reperfusion are indicated by dashed lines. The average pre-reperfusion ATP ratio in 60-min IRI group was used as the lowest ATP ratio because it was suggested to be the lowest ATP ratio in our experimental setting. IRI, ischemia reperfusion injury.

Supplementary Figure 4

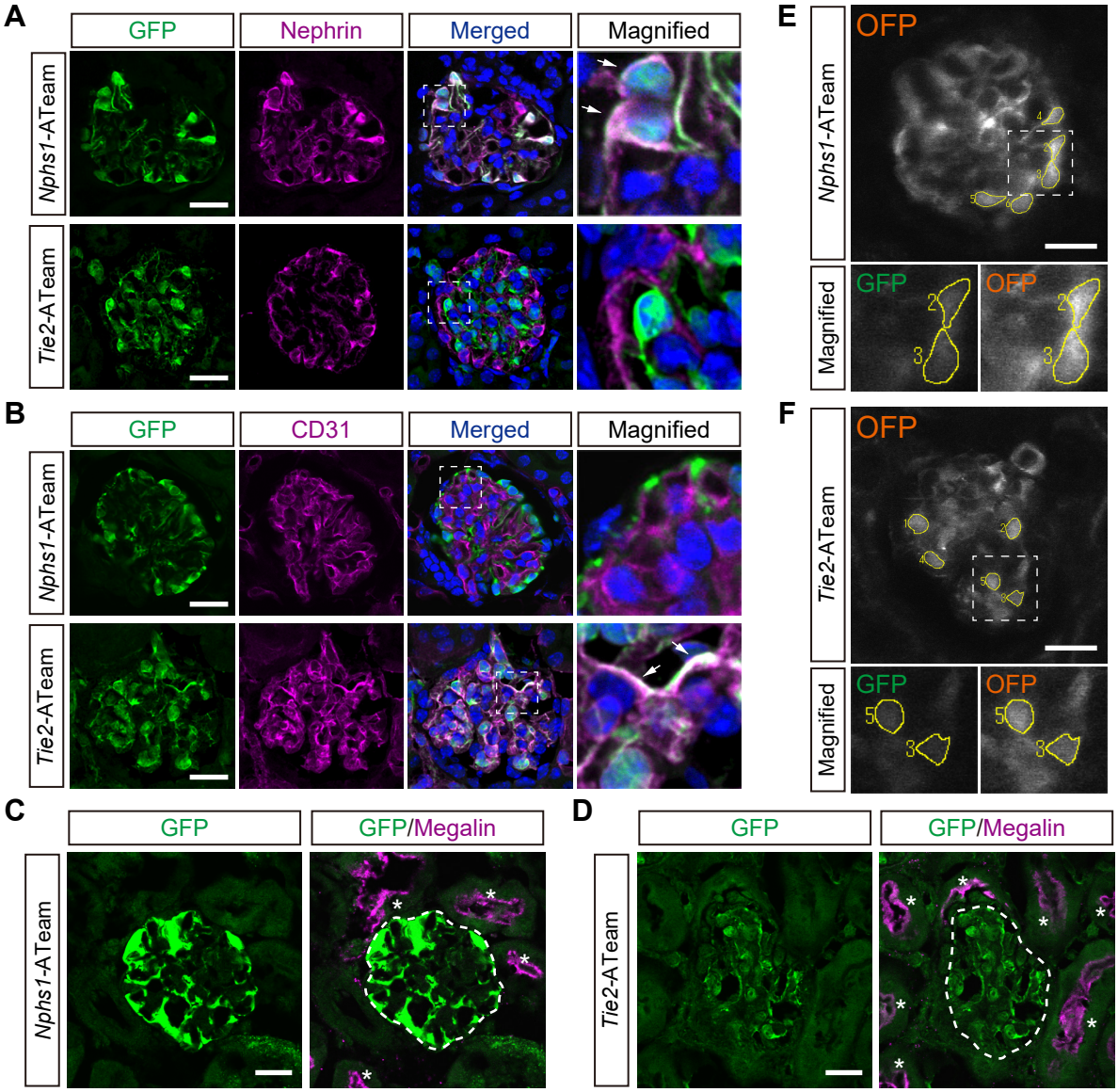

Supplementary Figure 4. Double staining of GO-ATeam2 biosensor and specific markers for glomerular cells in the *Nphs1*-ATeam and *Tie2*-ATeam glomerulus. (A) Confocal images of immunostaining of GO-ATeam2 biosensor and a podocyte marker nephrin in glomeruli from *Nphs1*-ATeam and *Tie2*-ATeam mice. Areas in the dashed boxes are magnified in the right panels. Arrows indicate podocytes. (B) Confocal images of immunostaining of GO-ATeam2 biosensor and an endothelial marker CD31 in glomeruli from *Nphs1*-ATeam and *Tie2*-ATeam mice. Areas in the dashed boxes are magnified in the right panels. Arrows indicate endothelial cells. (C) Confocal images of immunostaining of GO-ATeam2 biosensor and megalin, a marker for proximal tubules, in *Nphs1*-ATeam mice. Proximal tubules are indicated by asterisks. Glomerulus is segmented by a dashed line. (D) Confocal images of immunostaining of GO-ATeam2 biosensor and megalin in *Tie2*-ATeam mice. Proximal tubules are indicated by asterisks. Glomerulus is segmented by a dashed line. (E) Sample images of regions of interest in OFP and GFP images of *Nphs1*-ATeam mice. Regions of interest were created in OFP images and transferred to GFP images. The Area in the dashed box is magnified in the lower images. (F) Sample images of regions of interest in OFP and GFP images of *Tie2*-ATeam mice. Regions of interest were created in OFP images and transferred to GFP images. The Area in the dashed box is magnified in the lower images. Scale bars: 20 μm in A-F.

Supplementary Figure 5

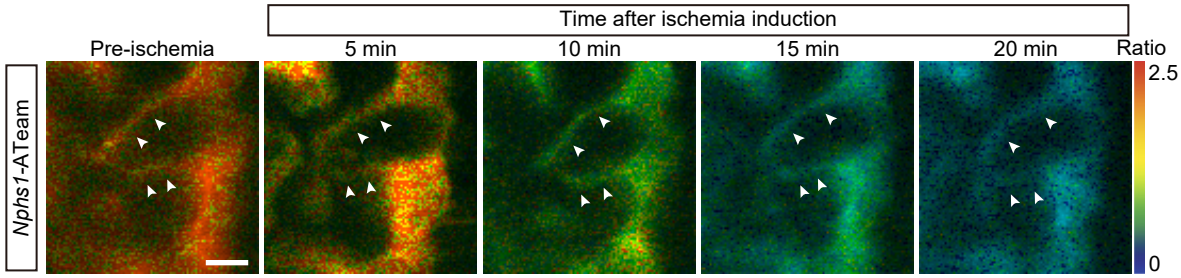

Supplementary Figure 5. ATP images of podocyte cellular processes of *Nphs1*-ATeam mice during ischemia. Arrowheads indicate podocyte cellular processes. Scale bars: 5 μm.

Supplementary Figure 6

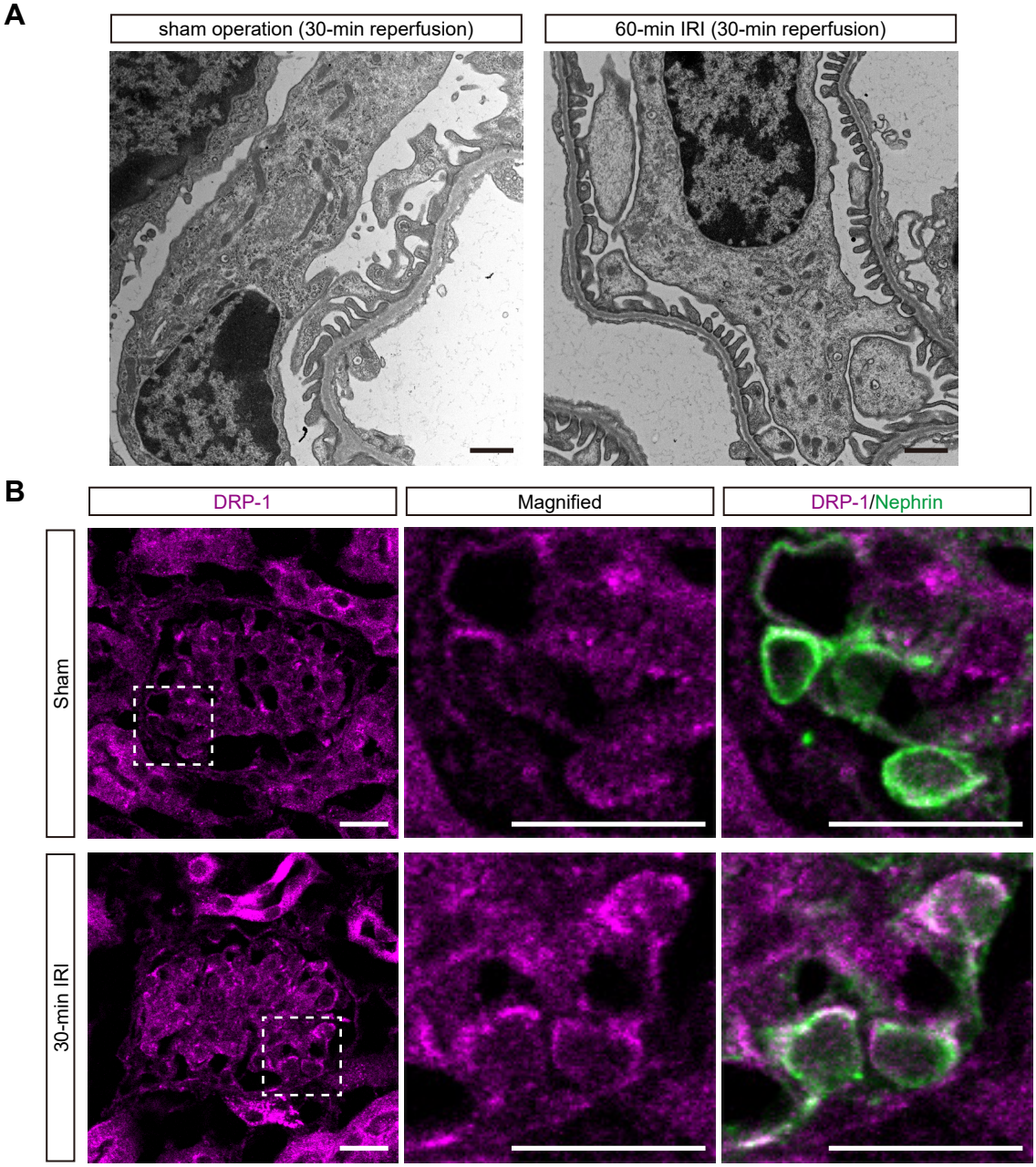

Supplementary Figure 6. Electron microscopic images of podocytes after 30-min reperfusion following 60-min IRI and DRP1 staining after 30-min IRI. (A) Electron microscopic images of podocytes after 30-min reperfusion following 60-min ischemia or sham surgery. Images are wider version of ones that are shown in Figure 6A. (B) DRP1 staining in glomeruli of wild type mice 1 hour after 30-minute IRI or sham surgery. The middle panels show magnified views of dashed boxes of the left panels. The right panels show co-localization of DRP1 and nephrin (green) in magnified views. Scale bars: 1 μm in A, 20 μm in B.

Supplementary Figure 7

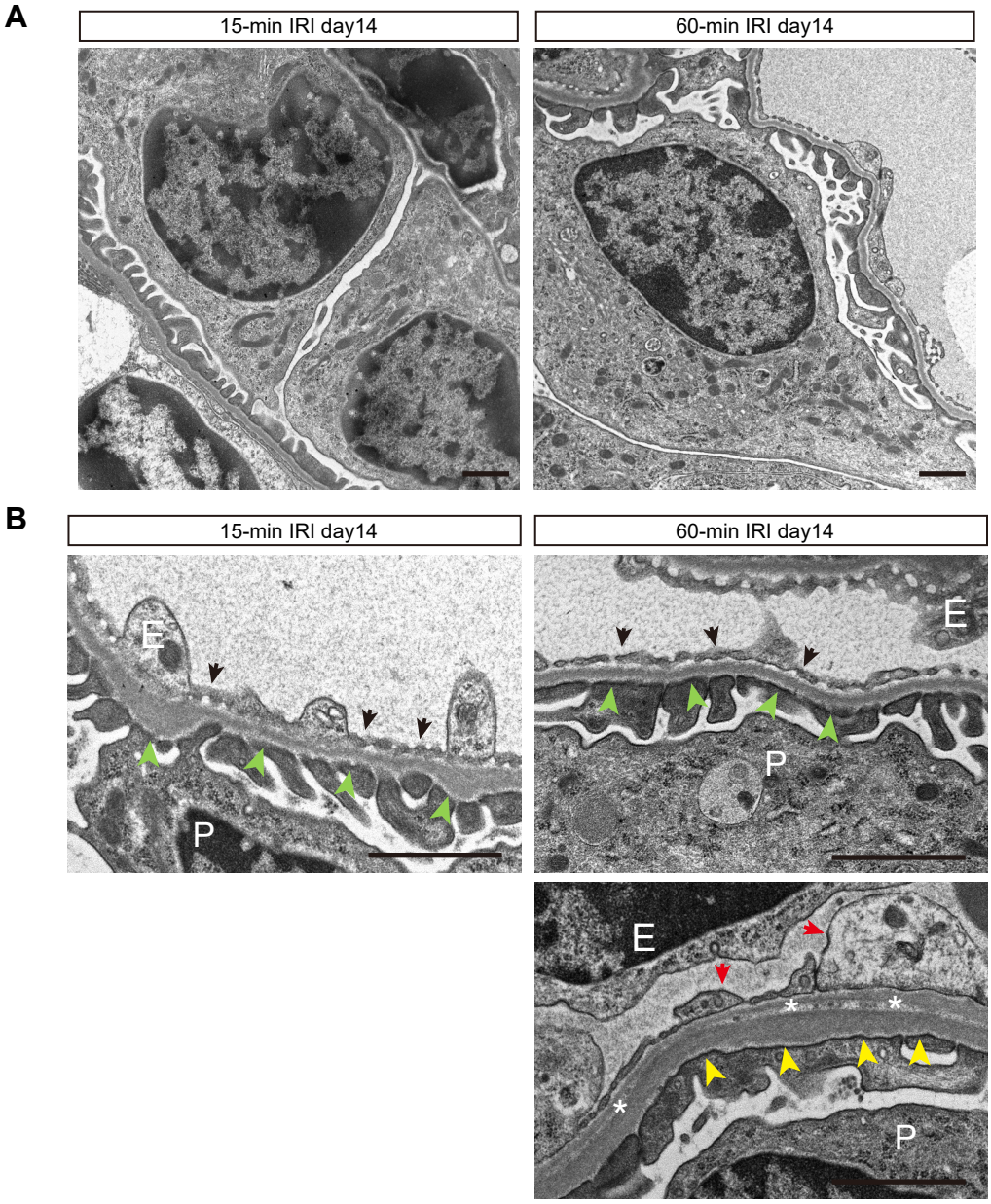

Supplementary Figure 7. Electron microscopic images of the glomerular capillary and the glomerular basement membrane 14 days after IRI. (A) Electron microscopic images of podocytes 14 days after 15-minute IRI or 60-minute IRI. Images are wider version of ones shown in Figure 7A. (B) Electron microscopic images of the glomerular capillary and the glomerular basement membrane 14 days after 15-min IRI or 60-minute IRI. Glomeruli after 15-minute IRI (left) showed the fine structure of endothelial fenestrations (black arrows) and the thin glomerular basement membrane (GBM, green arrowheads). In the glomeruli after 60-minute IRI, endothelial cells appeared generally normal with fine fenestrations (black arrows) and maintained GBM (green arrowheads) (upper right panel), while a limited number of glomeruli exhibited swollen endothelial cells (red arrows), thickened irregular GBM (yellow arrowheads), and GBM splitting (asterisks in the lower right panel). Scale bars: 1 μm in A and B. IRI, ischemia reperfusion injury; E, endothelial cell; P, podocyte.

Supplementary Table 1. Exact *p* values in Figure 8, C, D, F, and G

Exact *p*-value	Control vs Oligo + 2Dg
Figure 8C	$^{**}p$=0.0055
Figure 8D	$^{\#}p$=0.0302
Figure 8F	$^{*}p$=0.0006
Figure 8G	$^{**}p$=0.0020

*, p<0.001; **, p<0.01; $^{\#}$, p<0.05.

Oligo, oligomycin A; 2-Dg, 2-deoxy-D-glucose

Supplementary Table 2. Exact *p* values in Figure 8, I, J, L, and M

Exact *p*-value	Control + vehicle vs Oligo + 2Dg + vehicle	Control + vehicle vs Oligo + 2Dg + Mdivi-1	Oligo + 2Dg + vehicle vs Oligo + 2Dg + Mdivi-1
Figure 8I	$^{*}p$=0.0002	$^{\#}p$=0.0270	$^{\#}p$=0.0287
Figure 8J	$^{**}p$=0.0012	p=0.0547	$^{\#}p$=0.0217
Figure 8L	$^{*}p$<0.0001	$^{*}p$=0.0002	$^{\#}p$=0.0364
Figure 8M	$^{*}p$=0.0003	$^{**}p$=0.0047	$^{\#}p$=0.0366

*, p<0.001; **, p<0.01; $^{\#}$, p<0.05.

Oligo, oligomycin A; 2-Dg, 2-deoxy-D-glucose